J Chem Crystallogr (2015) 45:51–60
DOI 10.1007/s10870-014-0563-x

ORIGINAL PAPER

Two 1-(2-Furoyl)-3-phenylthiourea Derivatives: Synthesis, Characterization and Structural Study from X-ray Powder Diffraction Using Simulated Annealing

O. Estévez-Hernández · J. Rodríguez-Hernández · E. Reguera · J. Duque

Received: 3 July 2014 / Accepted: 17 December 2014 / Published online: 23 January 2015

Abstract 1-(2-furoyl)-3-*p*-cyanophenylthiourea (**1**) and 1-(2-furoyl)-3-*o*-fluorophenylthiourea (**2**) were synthesized by converting 2-furoyl chloride into 2-furoyl isothiocyanate and then condensing with the appropriated aniline derivatives. Both products were characterized by elemental analysis, Fourier transform infrared spectroscopy, Raman, ^{1}H, ^{13}C nuclear magnetic resonance and ab initio X-ray powder structure analysis. Compound **1** crystallizes in the monoclinic space group $P2_1/n$ with unit cell dimensions $a = 23.169(2)$ Å, $b = 11.353(2)$ Å, $c = 4.798(3)$ Å, $\beta = 90.30(2)°$, $V = 1{,}259.87(3)$ Å^3, $Z = 4$, $R_p = 4.62$, and $R_{wp} = 7.86$. Compound **2** crystallizes also in the monoclinic space group $P2_1/n$ with unit cell dimensions $a = 12.072(1)$ Å, $b = 20.801(2)$ Å, $c = 4.737(2)$ Å, $\beta = 93.34(2)°$, $V = 1{,}189.62(3)$ Å^3, $Z = 4$, $R_p = 3.95$, and $R_{wp} = 7.06$. The crystal structures have been determined from laboratory X-ray powder diffraction data using direct space global optimization strategy (simulated annealing) followed by the Rietveld refinement. The thiourea group makes a dihedral angle of 9.4(5)° and 33.5(4)° with the furoyl group in **1** and **2**, respectively. In both compounds, the *trans–cis* geometry of the thiourea unit is stabilized by intramolecular N–H···O hydrogen bond between the H atom of the *cis* thioamide and the carbonyl O atom. In the crystal structure of compound **1**, molecules are linked by intermolecular N–H···S bonds, forming one-dimensional chains along the *c* axis. For compound **2**, only Van der Waals interactions are observed in the crystal structure, forming one-dimensional chains along the *b* axis.

Graphical Abstract Crystal structure analysis from X-ray powder diffraction data and spectroscopic characterization of two 1-(2-furoyl)-3-phenylthiourea derivatives.

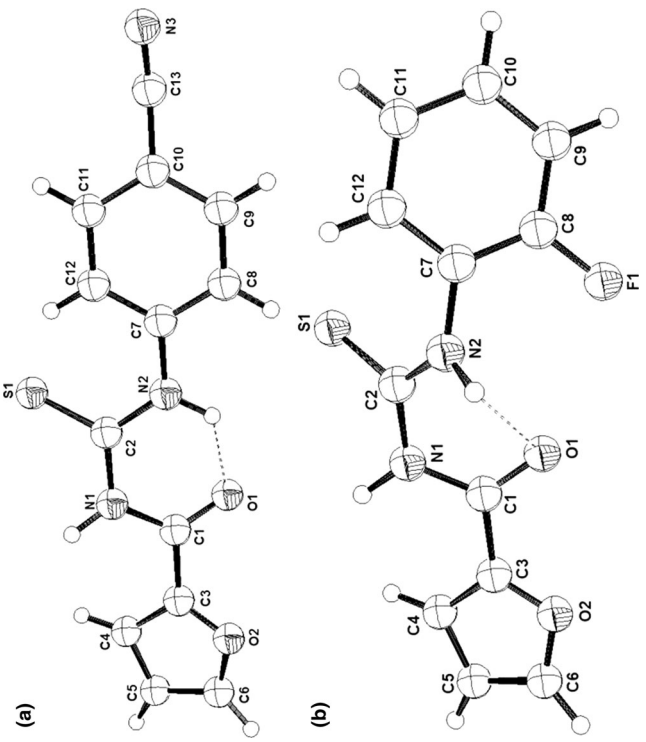

O. Estévez-Hernández · J. Duque (✉)
Instituto de Ciencia y Tecnología de Materiales (IMRE), Universidad de La Habana, Havana, Cuba
e-mail: jedv2013@gmail.com

J. Rodríguez-Hernández
Instituto de Investigaciones en Materiales, UNAM, Ciudad Universitaria, Circuito Exterior, 04510 Mexico, DF, Mexico

E. Reguera
Centro de Investigación en Ciencia Aplicada y Tecnología de Avanzada, IPN, Legaria 694, 11500 Mexico, DF, Mexico

Keywords Furoylthioureas · X-ray powder diffraction · Crystal structure · Simulated annealing · FTIR

Introduction

Thiourea derivatives have found extensive applications in the fields of medicine, agriculture and analytical chemistry [1]. Substituted thioureas are an important class of compounds, precursors or intermediates towards the synthesis of heterocyclic compounds [2–4]. Thioureas are also known to exhibit a wide range of bioactivities [5]. Thiourea derivatives are remarkable chelating agents for analytical chemistry and a variety of metal chelates have been described in literature [6, 7]. Over the past few years electrochemical sensors based in aroylthioureas as ionophores have been successfully developed and some basic approaches to describe the interaction mechanism of the ionophore with the heavy metal ion have been investigated [8–11]. Particularly, it has become a necessity to determine the structures as precisely as possible, since their shape and spatial fit with ions are important for good, sensible and selective electrodes [12]. The crystal structure of these versatile compounds is also important to understand its rich coordination chemistry [13]. For those materials for which it is complicated to grow single crystals, crystal structure resolution of molecular solids can nowadays be achieved from experimental X-ray diffraction (XRD) data combined with suitable softwares that apply Monte-Carlo/simulated annealing [14–18].

Following with our interest in the ion-recognition properties of 1-(2-furoylthiourea) derivatives, we report in this paper the spectroscopic characterization and crystal structure analysis from X-ray powder diffraction data of two 3-phenylmonosubstituted derivatives (**1** and **2**, see Scheme 1). They have strong electron-withdrawing substituents groups (*p*–C–N and *o*–F) in order to modulate the nucleophilic character of the C=S group as the main coordination center by the heavy metal ions.

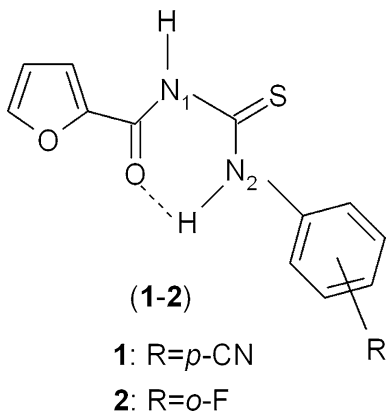

Scheme 1 Chemical diagram of compounds **1** and **2**

Experimental

Materials and Methods

All reagents and solvents for synthesis and analysis were commercially available and used as received without further purification. The melting point was determined with a Reichert-Jung rheostat coupled to a Reichert-Thermovar binoculars and a RS-3.722 digital thermometer. Elemental analyses were performed with a Leco automatic analyzer CHNS 932 model. The FTIR spectrum was recorded as KBr pellets on a Perkin Elmer Spectrum One FT-IR spectrometer in transmission mode with ten scans at a resolution of 2 cm^{-1}. Raman spectra were collected on a Horiba Jobin Yvon system LabRAM HR 800 and with HeNe (785 nm) laser. The laser power at the sample surface was 56.7 mW. The spectral bands pass of the Raman spectrometer was 1 cm^{-1}. ^{1}H and ^{13}C NMR spectra were obtained on a Bruker AC-250F spectrometer equipped with a computer ASPECT 3000 at frequencies of 250 MHz (^{1}H) and 62.89 MHz (^{13}C) at 25 °C. Sample (30 mmol/L) was dissolved in DMSO-d_6 (Aldrich). X-ray powder diffraction data was collected with a Bruker D8 Advanced diffractometer, equipped with a Lynxeye detector and CuKα1 radiation (1.54056 Å) at 25 °C.

Synthesis

(**1**) and (**2**) were synthesized as previously reported [8], by converting 2-furoyl chloride into 2-furoyl isothiocyanate and then condensing with the *p*-Cyanoaniline and *o*-Fluoroaniline, respectively. The solids precipitated were recrystallized from ethanol. Some of the synthetic and spectroscopic data for product (**1**) were previously published [19, 20].

*1-(2-Furoyl)-3-p-cya$_n$ophenylthiourea (**1**)*

Yield (98 %). Anal. Calcd for $C_{13}H_9N_3O_2S$: C 57.56, H 3.32, N 15.50, S 11.81 %; found: C 57.77, H 3.34, N 15.79 %, S 11.73 %.

Melting point (°C): 197–198.

IR spectrum [KBr] (cm^{-1}): ν_{max}/cm^{-1} 3399 ($N–H_{free}$), 3142–3098 (aromatic C–H), 3027 ($N–H_{assoc}$), 2226 (C–N), 1668 (C=O), 1598–1583 (aromatic C=C), 1549 [Thioamide band I, ν(C–N) + δ(NH)], 1341 [Thioamide band II, ν(C–N) + ν(C=S)], 1162 [Thioamide band III, ν(C–N) + ν(C=S)] and 773 [Thioamide band IV, ν(C=S)].

^{1}H NMR (DMSO-*d6*) δ 12.54 (1H, s, N2H), 11.47 (1H, s, N1H), 8.09 (1H, s, H_6), 8.01 (2H, d, H_8 and H_{12} of phenyl group), 7.89 (2H, d, H_9 and H_{11} of phenyl group), 7.87 (1H, d, H_4), and 6.77 (1H, dd, H_5); ^{13}C NMR (DMSO-*d6*) δ 178.8 (C=S), 157.3 (C=O), 148.5 (C_6), 144.6 (C_3), 142.1 (C_7), 132.8, (C_{10}), 124.2 (C_8), 118.8 (C_4), 118.5 (C_9), 112.6 (C_5).

*1-(2-Furoyl)-3-o-fluorophenylthiourea (**2**)*

Yield (92 %). Anal. Calcd for $C_{12}H_9N_2O_2SF$: C 54.54, H 3.41, N 10.61, S 12.12 %; found: C 54.67, H 3.24, N 10.79 %, S 12.43 %.

Melting point (°C): 155.

IR spectrum [KBr] (cm^{-1}): ν_{max}/cm^{-1} 3310 (N–H_{free}), 3161-3127 (aromatic C–H), 2975 (N–$H_{assoc.}$), 1677 (C=O), 1619-1567 (aromatic C=C), 1524 [Thioamide band I, ν(C–N) + δ(NH)], 1350 [Thioamide band II, ν(C–N) + ν(C=S)], 1166 [Thioamide band III, ν(C–N) + ν(C=S)] and 745 [Thioamide band IV, ν(C=S)].

^{1}H NMR (DMSO-*d6*) δ 12.33 (1H, s, N2H), 11.51 (1H, s, N_1H), 8.09 (1H, s, H_6), 8.01 (1H, t, H_9), 7.90 (1H, d, H_4), 7.36–7.33 (2H, m, H_{10} and H_{12}), 7.25 (1H, ddd, H_{11}), and 6.77 (1H, dd, H_5); ^{13}C NMR (DMSO-*d6*) δ 179.8 (C=S), 157.7 (C=O), 156.3 (C_8), 154.4 (C_7), 148.5 (C_6), 144.5 (C_3), 128.2 (C_9), 127.1, 126.1, 124.2 (C_{10}, C_{11}, C_{12}), 118.9 (C_4), 112.6 (C_5).

X-ray Data Collection and Structural Analysis

The samples were ground using agate pestle and mortar, and mounted in a top-loaded sample holder. X-ray powder diffraction data was recorded by a linear position-sensitive Lynxeye detector with a step size (2θ) of 0.008° and a counting time of 6 s (compound **1**) and 5 s (compound **2**) per step over an angular range of $5.0° < 2\theta < 90.0°$ using the Bragg–Brentano para-focussing geometry. Indexing of the X-ray powder pattern of **1** and **2** carried out using the program N-TREOR09 [21] indicated a monoclinic unit cell with $a = 23.169(2)$, $b = 11.353(2)$, $c = 4.798(3)$ Å and $\beta = 90.30(2)$ for **1** and a monoclinic unit cell with $a = 12.072(1)$, $b = 20.801(2)$, $c = 4.737(2)$ Å and $\beta = 93.34(2)$ for **2**. The figure of merits for **1** and **2** were $M(20) = 24$, $F(20) = 54$ and $M(20) = 19$, $F(20) = 33$, respectively. $P2_1/n$ space groups were determined on the basis of systematic absences. The full pattern decomposition was performed with EXPO2009 [21].

The Monte-Carlo structure determination method implemented in the program EXPO2009 [21] was used for solving the crystal structures of **1** and **2**. The molecular geometries used as input for structure solution were constructed using standard bond lengths and angles. The furan and benzene rings were maintained as rigid fragments. In the generation of trial structure during Monte-Carlo simulations, the structural fragment translation and rotation within the unit cell were carried out simultaneously with the intramolecular rotations. The molecular structure started with a typical two-dimensional drawing and it was transformed into a tri-dimensional structure. The initial position, orientation and intramolecular geometry of the structural fragment were chosen arbitrarily, and the random movement of the molecule in each Monte-Carlo move constrained such that the maximum displacement in any of the x, y, z coordinates (in orthogonal reference frame) was 0.5 Å and the maximum rotation of the molecules about three mutually perpendicular axes was ±45°. The scale factor functioning that is analogous to temperature in conventional Monte-Carlo simulations was fixed giving a 40.9 % acceptance of trial structure close to the optimum 40.0 %. Finally, after 437,000 trials, a structural model with $R_{wp} = 21.88$ was obtained.

The atomic coordinates obtained in the Monte-Carlo calculation were used as the starting model for the Rietveld refinement using the EXPO2009 [21] program package. In the final refinement all non-hydrogen atomic positions in the furan and benzene rings were restrained to the average values reported for analogous structures (1.380 Å). Removal of these restraints resulted in less satisfactory distances and angles without any improvement in the profile fit. For this reason, they were retained in refinements. The positions of all N, O and S isotropic atomic displacement parameters were refined. Hydrogen atoms were placed in the calculated positions using N–H = 0.96 Å and C–H = 0.96 Å (aromatic), but without effect on the refinement. Final Rietveld refinement converged to $R_p = 4.62$, $R_{wp} = 7.86$ for **1** (1,109 reflections) and to $R_p = 3.95$, $R_{wp} = 7.06$ for **2** (1,010 reflections), respectively.

Results and Discussion

X-ray Crystallography

The XRD patterns (experimental and calculated) of compounds **1** and **2** are shown in Fig. 1. Both structures suffer from less than adequate data to parameter ratios. This fact is reflected by a poor agreement of observed and calculated profiles, especially for compound **2**. Relevant crystallographic data of both compounds are summarized in Table 1. Atomic coordinates and equivalent isotropic displacement parameters are listed in Tables 2 and 3. Both compounds **1** and **2** crystallize in the thioamide form. The conformation of the molecules with respect to the carbonyl and thiocarbonyl part is non planar as reflected by the the torsion angles O1–C1–N1–C2, C1–N1–C2–S1, C1–N1–

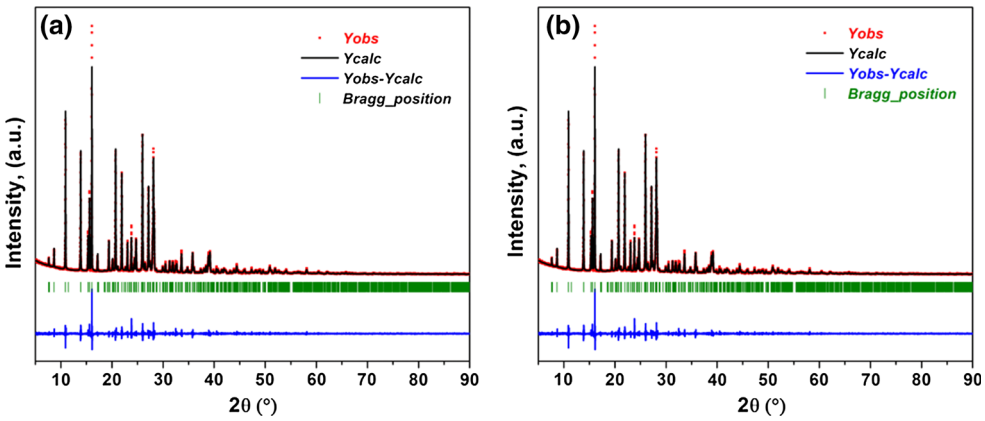

Fig. 1 Final Rietveld plot of **1** and **2**. *Red curve* observed pattern; *black curve* calculated pattern; *blue curve* difference curve; *green curve* background (Color figure online)

Table 1 Crystal data and Rietveld refinement parameters of compounds **1** and **2**

	1	**2**
Chemical formula	$C_{13}H_9N_3O_2S$	$C_{12}H_9N_2O_2SF$
Formula weight (M_r)	271.2	264.2
Crystal system, space group	Monoclinic, $P2_1/n$	Monoclinic, $P2_1/n$
Temperature (°K)	294 K	294 K
Unit cell dimensions		
a, b, c (Å)	23.169(2), 11.353(2), 4.798(3)	12.072(1), 20.801(2), 4.737(2)
β (°)	93.30(2)	90.34(1)
V (Å^3)	1,259.87(3)	1,189.62(3)
Z	4	4
Wavelength (Å)	1.54056	1.54056
D_{calc} (gcm^{-3})	1.430	1.475
2θ interval (°)	5.000–90.000	5.000–90.000
Step size (°), time (s)	0.008, 6	0.008, 5
No. of reflections	1,109	1,010
R_p	4.62	3.95
R_{wp}	7.86	7.06
S	1.70	1.79

C2–N2 of 9.0(8)°, 150.0(5)°, −28.0(8)° for **1** and 3.0(6)°, −140.2(4)°, 40.0(5)° for **2** respectively, closely related to other similar thiourea derivatives [22, 23]. In both compounds the benzoyl and phenyl groups are *trans* and *cis*, respectively to the S atom across the thiourea C–N bonds (Fig. 2). The main bond lengths and angles are given in Tables 4 and 5, and are between the ranges obtained for similar compounds from single-crystal data [12]. Generally for the compound refinement from powder data the distances are longer than those obtained from refinement with data collected using single-crystal. The C2–S1 and C1–O1 bonds show typical double-bond character with bond lengths of 1.60(6), 1.22(6) Å and 1.61(5), 1.20(5) Å for **1** and **2**, respectively. Particularly, the C2–S1 distance around 1.60–1.61 Å is shorter than that reported for related compounds from single-crystal data. All the C–N bonds of thiourea fragment C1–N1, C2–N1 and C2–N2 are in the range 1.37–1.39 Å, intermediate between those expected for single and double C–N bonds (1.47 and 1.27 Å respectively). These results can be explained by the existence of resonance in this part of the molecule. The central thiourea fragment (N1–C2–S1–N2) makes dihedral angles of 9.4(5)° and 33.5(4)° with the furan carbonyl (O1–O2–C1–C3) group, whereas the C7–C12 benzene rings are inclined by 11.1(2)° and 50.7(2)° in **1** and **2**, respectively. In this conformation the sulfur and oxygen atoms are in the so called *quasi*-S form [24]. The molecules **1** and **2** are further stabilized by intramolecular and intermolecular hydrogen bonding. In both compounds, the *trans–cis* geometry of the thiourea unit is stabilized by intramolecular N2–H1···O1 hydrogen bonds. As a result, a pseudo six membered (O1–C1–N1–C2–N2···H2) ring is formed (Fig. 2). In the crystal structure of compound

Table 2 Positional and displacement parameters of compound **1**

Atoms	*x*	*y*	*z*	U_{iso}*/U_{eq}	Occ.
C3	0.748(2)	0.164(5)	0.382(2)	0.058(2)	1.00000
C4	0.770(3)	0.055(5)	0.454(4)	0.058(2)	1.00000
O2	0.767(5)	0.240(7)	0.542(3)	0.058(2)	1.00000
C6	0.801(3)	0.200(1)	0.721(3)	0.058(2)	1.00000
C5	0.806(4)	0.080(3)	0.684(6)	0.058(2)	1.00000
C1	0.707(4)	0.164(5)	0.164(5)	0.058(2)	1.00000
O1	0.801(3)	0.186(5)	0.144(3)	0.058(2)	1.00000
N1	0.801(3)	0.164(5)	0.164(5)	0.058(2)	1.00000
C2	0.634(3)	0.116(4)	−0.185(3)	0.058(2)	1.00000
S1	0.611(4)	0.003(3)	−0.356(3)	0.058(2)	1.00000
N2	0.622(5)	0.228(6)	−0.286(4)	0.058(2)	1.00000
C7	0.580(1)	0.248(6)	−0.504(2)	0.058(2)	1.00000
C10	0.498(2)	0.292(2)	−0.936(7)	0.058(2)	1.00000
C11	0.510(5)	0.177(4)	−0.855(3)	0.058(2)	1.00000
C9	0.526(5)	0.384(3)	−0.801(6)	0.058(2)	1.00000
C12	0.551(6)	0.155(2)	−0.640(3)	0.058(2)	1.00000
C8	0.567(4)	0.363(3)	−0.585(3)	0.058(2)	1.00000
C13	0.456(3)	0.314(5)	−1.157(6)	0.058(2)	1.00000
N3	0.418(6)	0.328(4)	−1.325(3)	0.058(2)	1.00000

Hydrogen atoms were placed in the calculated positions using N–H = 0.96 Å and C–H = 0.96 Å (aromatic)

Table 3 Positional and displacement parameters of compound **2**

Atoms	*x*	*y*	*z*	U_{iso}*/U_{eq}	Occ.
C3	0.739(2)	−0.034(5)	0.035(1)	0.038(2)	1.00000
C4	0.644(3)	−0.068(5)	−0.017(4)	0.038(2)	1.00000
O2	0.813(2)	−0.049(3)	−0.123(6)	0.038(2)	1.00000
C6	0.783(3)	−0.091(4)	−0.287(4)	0.038(2)	1.00000
C5	0.674(3)	−0.107(2)	−0.237(3)	0.038(2)	1.00000
C1	0.750(4)	0.015(3)	0.256(2)	0.038(2)	1.00000
O1	0.840(2)	0.029(4)	0.347(6)	0.038(2)	1.00000
N1	0.657(3)	0.045(1)	0.360(2)	0.038(2)	1.00000
C2	0.668(3)	0.093(2)	0.558(6)	0.038(2)	1.00000
S1	0.582(5)	0.097(2)	0.815(5)	0.038(2)	1.00000
N2	0.752(5)	0.137(4)	0.536(6)	0.038(2)	1.00000
C7	0.791(1)	0.173(6)	0.769(6)	0.038(2)	1.00000
C10	0.869(5)	0.243(5)	1.226(1)	0.038(2)	1.00000
C11	0.759(4)	0.249(3)	1.142(7)	0.038(2)	1.00000
C9	0.940(3)	0.203(3)	1.081(2)	0.038(2)	1.00000
C12	0.720(4)	0.214(2)	0.914(3)	0.038(2)	1.00000
C8	0.901(1)	0.168(2)	0.853(4)	0.038(2)	1.00000
F1	0.968(3)	0.129(3)	0.714(4)	0.038(2)	1.00000

Hydrogen atoms were placed in the calculated positions using N–H = 0.96 Å and C–H = 0.96 Å (aromatic)

1, molecules are linked by intermolecular N1–H1···S1 bonds, forming one-dimensional chains along the *c* axis (Fig. 3), whereas for compound **2**, only Van der Waals interactions are observed in the crystal structure, forming one-dimensional chains along the *b* axis (Fig. 4). This fact is probably due to the influence of a strong electron-withdrawing group as –F, in proximity to the S atom.

FTIR-Raman spectroscopy

The main FTIR-Raman frequencies and their assignments are summarized in Table 6. The FTIR spectra of the compounds studied showed two peaks due to, N–H vibrations centered at 3,399/3,027 cm^{-1} and 3,310/2,975 cm^{-1} for (**1**) and (**2**), respectively. The peaks at

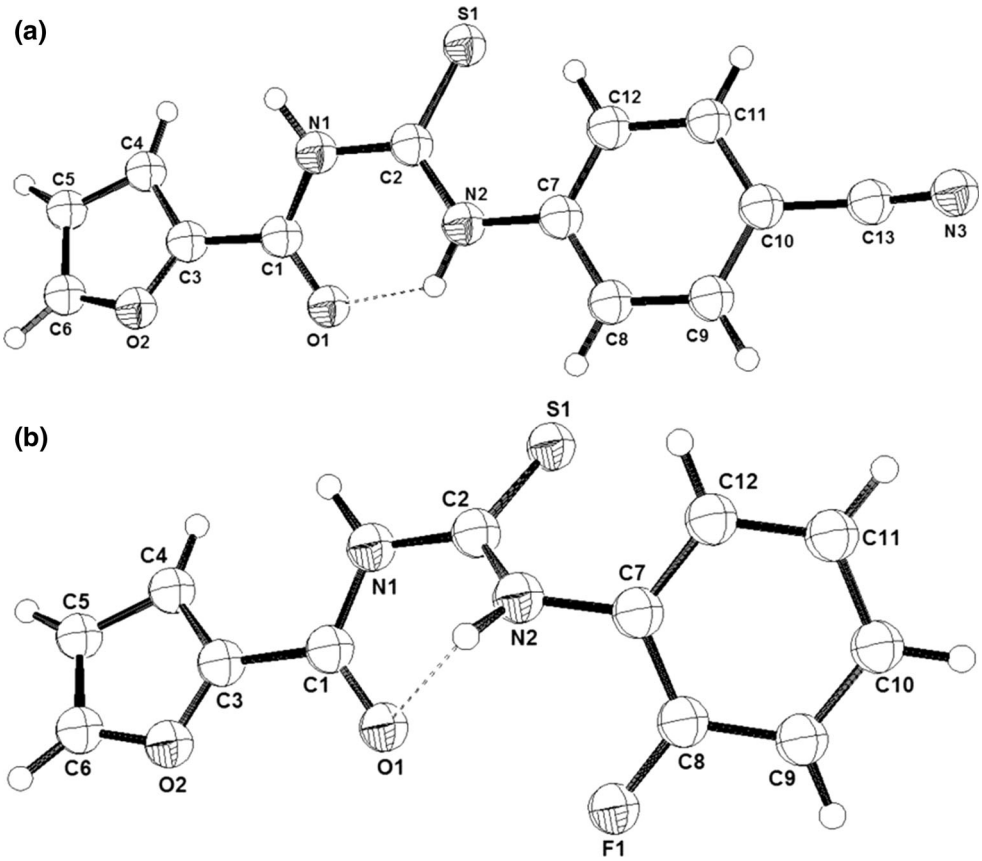

Fig. 2 View of the asymmetric units of **1** (**a**) and **2** (**b**) with atom numbering scheme (50 % probability displacement ellipsoids)

higher frequencies are assigned to N1–H stretching (involves weakly associated hydrogen atoms). The much lower frequencies assigned to N2–H motions (sharper peaks) show the pronounced effect of association for these hydrogen atoms that are forming strong intramolecular hydrogen bonding with carbonylic oxygen. This effect is especially pronounced for compound **2**. The presence of a highly electronegative group (–F) in *ortho* position of the phenyl group seems to strengthen the intramolecular hydrogen bond. In the 3,500-2,500 cm^{-1} region stretches of N–H group vibrations are merged with those of C–H stretching from furoyl and phenyl groups, making difficult an accurate assignment of these peaks. For that reason we have made the ν(N–H) assignments based on both spectra FTIR and Raman. This methodology has been used in previous reports [7, 25]. Concerning to the number of bands and their frequency, the Raman spectrum seems to be a reflection of the corresponding IR one and vice versa. However, regarding their intensity, these spectra are quite different. In Raman, the combination bands do not occur with significant intensity, particularly those bands involving bending modes of light atoms (e.g., H) due to their relatively small polarizability. For compound **1**, there is a very weak band at 3,400 cm^{-1} ascribed to N1–H stretching while it is not assignable the N2–H stretching, since it is probably submerged by the several most intense bands related to aromatic C–H stretchings (see Fig. 5a). However, for compound **2** the frequencies of N2–H and aromatic C–H stretchings are more separated probably due to the above-mentioned effect of a very electronegative group as –F in *ortho* position at the phenyl group. There bands involving ν(N–H) motions in the Raman spectrum of this later compound (see Fig. 5b) are not assignable. This fact allows the unequivocal assigning of the weak peaks in the 3,143–3,054 cm^{-1} region (with counterparts at 3,161–3,127 cm^{-1} in the FTIR spectrum) as aromatic C–H stretching. This assignment is not in agreement with previous reports concerning vibrational studies of aroylthiourea derivatives [7, 25]. The strong peaks observed at 1,668 cm^{-1} (**1**) and 1,677 cm^{-1} (**2**) correspond to C=O stretching. The aromatic C=C stretching frequency bands appear at 1,610–1,580 cm^{-1} for both compounds, while the most intense peaks at 1,549/1,524, 1,341/1,350 and 1,161/1,166 cm^{-1} can be assigned to Thioamide bands I [ν(C–N) + δ(NH)], II [ν(C–N) + ν(C=S)] and III [ν(C–N) + ν(C=S)] for (**1**)/(**2**), respectively. The band ascribed to Thioamide band IV [mainly ν(C=S)] is difficult to assign in the FTIR spectra of thiourea derivatives. This usually weak band emerges in a region which is rich in

Table 4 Selected bond lengths (Å) and bond angles (°) of compound **1**

C1–C3	1.47(7)	C7–N2	1.41(8)
C1–O1	1.22(6)	C8–C9	1.39(9)
C1–N1	1.37(9)	C9–C10	1.37(7)
C2–N1	1.38(6)	C10–C11	1.39(5)
C2–N2	1.39(8)	C11–C12	1.39(12)
C2–S1	1.60(6)	C13–C10	1.42(6)
C3–C4	1.38(8)	C13–N3	1.17(11)
C3–O2	1.22(8)		
C4–C5	1.38(7)		
C5–C6	1.38(4)		
C6–O2	1.22(9)		
C7–C8	1.39(7)		
C7–C12	1.40(8)		
C3–C1–O1	119(6)	C7–C8–C9	120(2)
C3–C1–N1	120(3)	C8–C9–C10	121(3)
O1–C1–N1	121(4)	C9–C10–C11	120(3)
N1–C2–N2	120(2)	C10–C11–C12	120(5)
N1–C2–S1	120(2)	C7–C12–C11	120(2)
N2–C2–S1	120(4)	C8–C7–C12	119(4)
C1–C3–C4	124(3)	C8–C7–N2	119(5)
C1–C3–O2	124(6)	C12–C7–N2	121(6)
C4–C3–O2	111(5)	C13–C10–C9	120(3)
C3–C4–C5	102(2)	C13–C10–C11	120(3)
C4–C5–C6	105(3)	N3–C13–C10	120(3)
		C5–C6–O2	110(4)

Table 5 Selected bond lengths (Å) and bond angles (°) of compound **2**

C1–C3	1.46(8)	C7–N2	1.41(9)
C1–O1	1.20(5)	C8–C9	1.38(4)
C1–N1	1.38(6)	C9–C10	1.38(8)
C2–N1	1.38(4)	C10–C11	1.39(7)
C2–N2	1.37(8)	C11–C12	1.38(5)
C2–S1	1.61(5)	C8–F1	1.33(5)
C3–C4	1.37(8)		
C3–O2	1.21(4)		
C4–C5	1.37(7)		
C5–C6	1.38(6)		
C6–O2	1.22(8)		
C7–C8	1.39(2)		
C7–C12	1.39(9)		
C3–C1–O1	120(5)	C7–C8–C9	120(4)
C3–C1–N1	120(4)	C8–C9–C10	120(3)
O1–C1–N1	120(4)	C9–C10–C11	120(3)
N1–C2–N2	120(3)	C10–C11–C12	120(3)
N1–C2–S1	120(2)	C7–C12–C11	120(3)
N2–C2–S1	120(3)	C7–C8–F1	119(2)
C1–C3–C4	124(2)	C9–C8–F1	120(2)
C1–C3–O2	124(5)		
C4–C3–O2	112(6)		
C3–C4–C5	102(2)		
C4–C5–C6	104(2)		

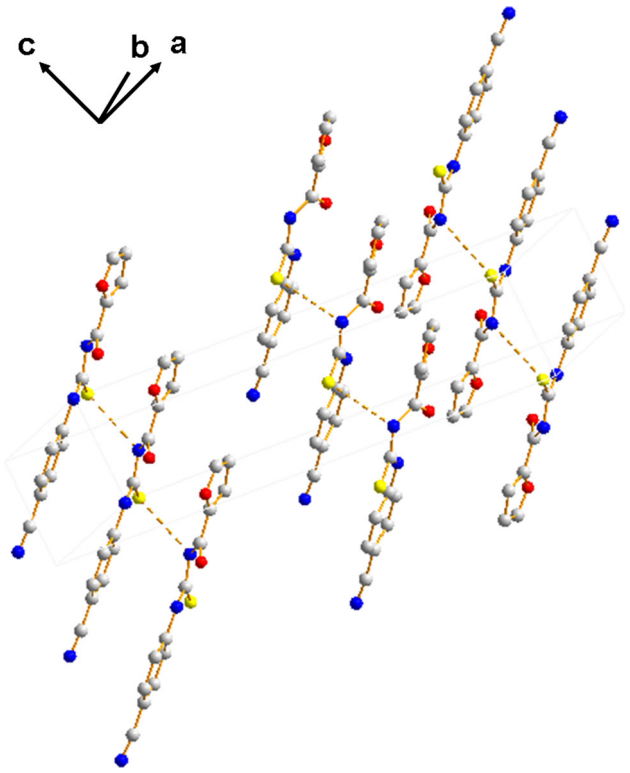

Fig. 3 View of the crystal packing of the compound **1**

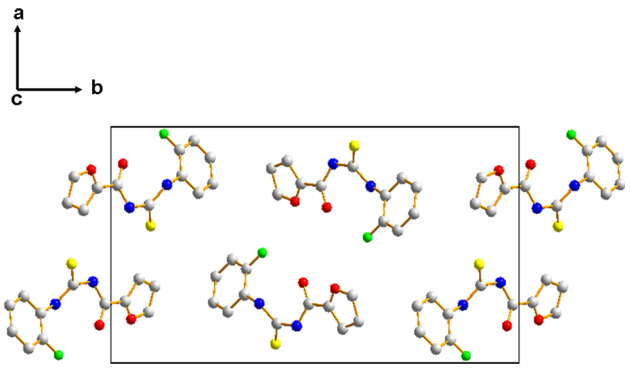

Fig. 4 View of the crystal packing of the compound **2**

absorptions from skeletal motions within the substituent groups and makes their identification difficult. Signals from motions of atoms as sulfur with highly polarizable electronic structure appear with relatively high intensity in the Raman spectra. This fact has been used to identify the C=S stretching comparing IR and Raman spectra of each compound (see Fig. 6). The peaks at 773 and 745 cm^{-1} (770 and 742 cm^{-1} Raman) were ascribed to the ν(C=S) mode for (**1**) and (**2**), respectively. This assignment is in agreement with previously studied thiourea derivatives [7, 25, 26].

^{1}H and ^{13}C NMR spectroscopy

In DMSO-d_6, the two most de-shielded signals for both compounds were broad. They were assigned to NH protons [20]. The N1H proton is acidic and shows a strong solvating effect due to DMSO. Usually, their δ^{1}H values are in the range of 11–12 ppm. For the title compounds (**1**) and (**2**) the chemical shifts of N1H protons are 11.47 and 11.51 ppm, respectively. As a rule, in most 3-substituted aroylthioureas with aromatic substituent at N2, this hydrogen bonded N2H proton has the higher δ^{1}H value between 12 and 13 ppm. This fact is observed for both studied compounds with chemical shifts for N2H protons of 12.54 (**1**) and 12.33 (**2**) ppm, respectively. The effect of strong electron-withdrawing substituent (–C–N and –F) groups in the phenyl ring on the N1H and N2H chemical shifts is not significant as reported by Macías et al. [27]. For the compounds related, there have been reported lower δ^{1}H values in $CDCl_3$ and DMSO-d_6 (8–10 ppm) due the presence of strong electron-withdrawing substituent groups in the aroyl [20] or 3-monosubstitutedphenyl [28] fragments. The furan protons (8.09–6.77 ppm) show a similar, typical spin system of a carbonyl substituted furan for both compounds. These signals are not sensitive to the electronic effects by the substituents in N. The protons of the resonant phenyl groups appear in down fields of δ = 8.01–7.87 ppm for (**1**) and δ = 8.01–7.25 ppm for

Table 6 FTIR and Raman spectral mode assignments of compounds **1** and **2**

	1		**2**	
Assignment	FTIR	Raman	FTIR	Raman
ν(N–H)$_{free}$	3,399	3,400	3,310	Not assignable
ν(C–H)$_{aromatic}$	3,142−3,068	3,144–3,056	3,161–3,127	3,143–3,054
ν(N–H)$_{assoc}$	3,027	Not assignable	2,975	Not assignable
ν(C=O)	1,668	1,666	1,677	1,678
ν(C=C)$_{aromatic}$	1,598–1,583	1,608–1,581	1,619–1,567	1,615–1,557
Thioamide I	1,549	1,548	1,524	1,527
Thioamide II	1,341	1,341	1,350	1,351
Thioamide III	1,162	1,161	1,166	1,167
Thioamide IV	773	770	745	742

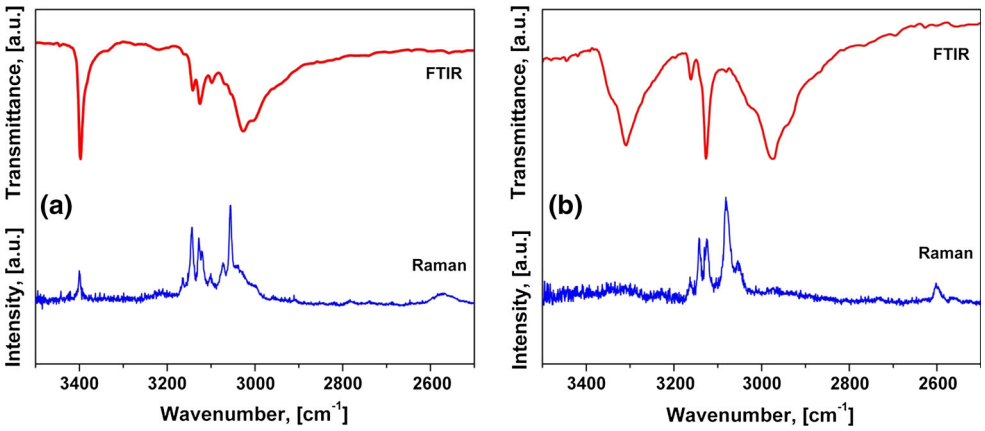

Fig. 5 FT-IR and Raman spectra of compounds **1** (**a**) and **2** (**b**) in the 3,500–2,500 cm^{-1} region, where the N–H stretching vibrations appear

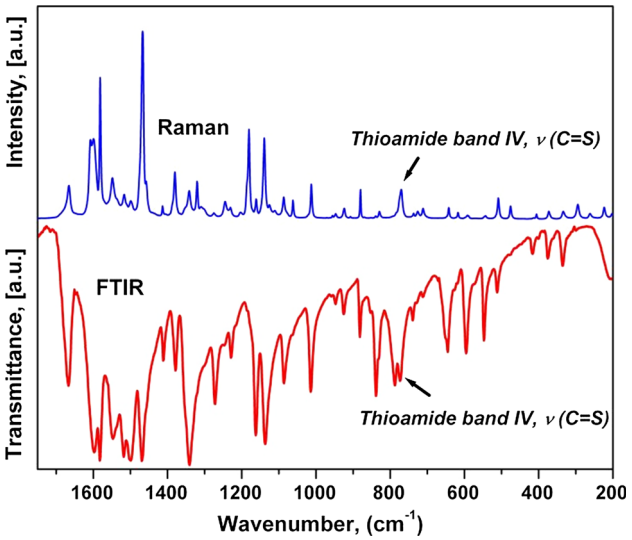

Fig. 6 FT-IR and Raman spectra of compound **1** in the 1,750-200 cm^{-1} region. The C=S stretching vibration appears at 773 and 770 cm^{-1}, respectively

(**2**). The ^{13}C NMR spectra show the C=S/C=O signals for (**1**) at (**2**) at 178.8/157.1 and 179.8/157.7 ppm, respectively. Usually, for the 3-monosubstituted derivatives the C=S group is less affected than in the 3,3-disubstituted compounds due to the intramolecular hydrogen bond between the N2H proton and the carbonylic oxygen of the aroyl group. This fact inhibits the drastic paramagnetics changes caused by the free rotation in the thioamidic moiety comprising the N2 atom for 3,3-disubstituted derivatives. For the C=O group the effect is even lower. Similar to that observed for the furan protons, the furan carbon are almost not affected by the substituents in N2.

Conclusion

Two 1-(2-furoyl)-3-phenylthiourea derivatives were prepared. Compound **2** is first reported. FTIR and Raman vibrational spectroscopic properties were investigated. The crystal structure is similar for both compounds and was determined using X-ray powder diffraction method and Monte-Carlo Simulated Annealing technique. A strong C=O···H–N intramolecular hydrogen bond locks the molecules in a pseudo six membered (O–C–N–C–N···H) ring. This hydrogen interaction is also confirmed in solution from NMR studies. In the crystal structure of compound **1**, molecules are linked by intermolecular N–H···S bonds. For compound **2**, only Van der Waals interactions are observed.

Supplementary Material

The crystallographic information file (abbreviated CIF) loading the data sets (excluding the structure factors) for compounds **1** and **2** has been deposited with the Cambridge Structural Data Base, under deposit codes CCDC 928748 and CCDC 928747, respectively (copies of these data may be obtained free of charge from The Director, CCDC, 12 Union Road, Cambridge CB2 1EZ, UK, Fax: ± 44 1223 336033; Email: deposit@ccdc.cam.ac.uk or http://www.ccdc.ac.uk).

Acknowledgments JD acknowledge the financial support from Consejo Nacional de Ciencia y Tecnología (CONACyT), México. "Programa de Estancias Posdoctorales y Sabáticas al Extranjero para la Consolidación de Grupos de Investigación", No de Propuesta: 203824.

References

1. Aly AA, Ahmed EK, El-Mokadem KM, Hegazy MEF (2007) J Sulfur Chem 28:73–93
2. Jain VK, Rao JT (2003) J Inst Chem 75:24–26
3. Ďhooghe M, Waterinckx A, De Kimpe N (2005) J Org Chem 70:227–232
4. Zeng RS, Zou JP, Zhi SJ, Chen J, Shen Q (2003) Org Lett 5:1657–1659

5. Saeed S, Rashid N, Jones PG, Ali M, Hussain R (2010) Eur J Med Chem 45:1323–1331
6. Saeed S, Rashida N, Wong WT (2010) Acta Cryst E 66:o1031–o1032
7. Estévez-Hernández O, Otazo-Sánchez E, Hidalgo-Hidalgo de Cisneros JL, Naranjo-Rodríguez I, Reguera E (2006) Spectrochimica Acta Part A 64:961–971
8. Otazo-Sánchez E, Pérez-Marín L, Estévez-Hernández O, Rojas-Lima S, Alonso-Chamorro J (2001) J Chem Soc Perkin Trans II:2211–2218
9. Wilson D, Arada MA, Alegret S, Del Valle M (2010) J Hazard Mater 181:140–146
10. Lazo-Fraga AR, Collins A, Forte G, Rescifina A, Punzo F (2009) J Mol Struct 929:174–181
11. Lazo-Fraga AR, Li Destri G, Forte G, Rescifina A, Punzo F (2010) J Mol Struct 981:86–92
12. Estévez-Hernández O, Duque J, Reguera E (2011) J Sulfur Chem 32:213–222
13. Koch KR (2001) Coord Chem Rev 216–217:473–488
14. Bruker Company, AXS, TOPAS; Bruker AXS: Karlsruhe, Germany, 1997
15. Fujii K, Garay AL, Hill J, Sbircea E, Pan Z, Xu M, Apperly DC, James SL, Harris KDM (2010) Chem Commun 46:7572–7574
16. Ibberson RM, Fowkes AJ, Rosseinsky MJ, David WIF, Edwards PP (2009) Angew Chem Int Ed 48:1435–1438
17. Das U, Chattopadhyay B, Mukherjee M, Mukherjee AK (2012) Cryst Growth Des 12:466–474
18. Chattopadhyay B, Ghosh S, Mondal S, Mukherjee M, Mukherjee AK (2012) CrystEngComm 14:640–647
19. Otazo-Sánchez E, Ortiz-del-Toro P, Estévez-Hernández O, Pérez-Marín L, Goicoechea I, Cerón-Beltrán A, Villagómez-Ibarra JR (2002) Spectrochimica Acta Part A 58:2281–2290
20. Estévez-Hernández O, Otazo-Sanchez E, Hidalgo-Hidalgo de Cisneros JL, Naranjo-Rodriguez I, Reguera E (2005) Spectrochimica Acta. Part A 62:964–971
21. Altomare A, Camalli M, Cuocci C, Giacovazzo C, Moliterni A, Rizzi R (2009) J Appl Crystallogr 43:798–804
22. Theodoro JE, Mascarenhas Y, Ellena J, Estévez-Hernández O, Duque J (2008) Acta Crystallogr E 64:o1193
23. Corrêa RS, Estévez-Hernández O, Ellena J, Duque J (2008) Acta Crystallogr E 64:o1414
24. Plutin AM, Marquez H, Ochoa E, Morales M, Sosa M, Moran L, Rodríguez Y, Suarez M, Martín N, Seoane C (2000) Tetrahedron 56:1533–1539
25. Saeed A, Erben MF, Bolte M (2013) Spectrochimica Acta Part A 102:408–413
26. Yang W, Zhou W, Zhang Z (2007) J Mol Struct 828:46–53
27. Macías A, Otazo E, Pita G, Gra R, Beletskaia IP (1982) Zhur Org Jimii 8:905–909
28. Zhu W, Yang W, Zhou W, Liu H, Wei S, Fan J (2011) J Mol Struct 1004:74–81